

DIRECT BED STRESS MEASUREMENTS UNDER SOLITARY TSUNAMI-TYPE WAVES AND BREAKING TSUNAMI WAVE FRONTS

Jaya Kumar Seelam¹ and Tom E. Baldock²

Abstract

During their propagation tsunamis often traverse continental slopes that are relatively steep compared to deeper oceans. Further due to the change of bed slope from offshore to near shore, there is every likely possibility that a tsunami might steepen and eventually break, thereby generating large pressure gradients that could enhance the likelihood of liquefaction of the seabed. In the drawdown, high shear stresses could trigger debris flow in submarine canyons and on steep ridges. Therefore estimation of the bed stress is important in estimation of the forces induced during tsunami wave propagation, both on the seabed as well as on the subsurface installations. Bed and shear stresses generated by wave forms that represent tsunami (a solitary wave and broken solitary wave in the form of a bore) are measured using a shear cell. This paper deals with the measurements and modeling of the bed stress under the solitary waves.

Key words: hydrodynamics, tsunami, shear stress, shear plate, continental slope, liquefaction

1. Introduction

Tsunamis are long waves of small steepness, generated by impulsive geophysical events of the seafloor and of the coastline, such as subsea earthquakes, submarine and aerial mass failures, volcanic eruptions and asteroid impacts (Synolakis and Bernard, 2006). Tsunamis often result in enormous damage to communities as well as to coastal infrastructure. Apart from coastal infrastructure, offshore facilities are also vulnerable to tsunamis, especially offshore oil & gas installations such as marine risers, shore connecting pipelines and associated structures. Changes in the seabed that are associated with the tsunami are seldom reported due to the difficulties in ascertaining the regional extent of the instability and the importance of the study region. Deep ocean pipelines routing up the continental slope with changing bathymetry are vulnerable to hazards derived from extreme events like Tsunamis. Tsunami loading on offshore pipelines is not often considered in the design process and also the resultant bed dynamics are poorly reported. Very little information on the breaking of tsunamis is available in literature. Measurements of shear stresses under wave forms representing tsunami are scarce and they are reported to be difficult to measure (Liu et al., 2007) and thus any measurements in this regard are valuable. Ippen and Mitchell (1957) have presented direct measurements of shear stresses in a wave flume using a shear plate that measured force and this method was termed as intrusive and hence the data was of poor quality (Liu et al., 2007). Indirect methods are mostly used to measure the velocity profile in the boundary layer and the shear stresses is further estimated from the velocity profile (Gislason, 2009, Holmedal et al., 2003, Huang and Dong, 2001, Liang et al., 2008, Lin and Zhang, 2008, Liu et al., 2007, Liu et al., 2006). Hot film probes have been employed to measure the bed shear stress on a smooth bed in U tube experiments by Jensen et al (1989). Laser Doppler Velocimeter (LDV) has been used in several oscillatory bottom boundary layer experiments (Jensen et al., 1989, Liu et al., 1996, Sleath, 1987, Sumer et al., 1993). Another non-intrusive technique adopted is the particle image velocimetry (PIV) which provides whole-field measurements. Several studies are carried out using PIV technique (Chang and Liu, 1998, Chang and Liu, 1999, Cowen and Monismith, 1997, Cowen et al., 2003, Lin and Rockwell, 1994, Lin and Rockwell, 1995). Although the direct measurement of shear stress using a shear plate by Ippen & Mitchel (1957) was

¹Dept of Civil Eng., The University of Queensland, St Lucia, QLD 4072, Australia. j.seelam@uq.edu.au; Also at National Institute of Oceanography (CSIR - INDIA), Dona Paula, Goa, India. jay@nio.org.

²Dept of Civil Eng., The University of Queensland, St Lucia, QLD 4072, Australia. t.baldock@uq.edu.au.

referred as intrusive method by Liu et al (2007), the observations from shear cells are consistent with those from non-intrusive methods, thus verifying the fact that shear plate measurements do provide the required and relevant information. Ippen & Mitchell (1957) used a force gauge rigidly mounted above the wave channel. The force gauge transducer was based on linear differential transformer which measured the horizontal deflection of the shear plate, the deflection being proportional to the force applied. These measurements were one of the first measurements reported and probably the earliest available direct shear stress measurements in the literature for solitary waves. Shear plates have been used to measure the shear stress due to waves in different regions. Recent studies include Barnes and Baldock (2007) and Barnes et al. (2009) wherein they studied flows due to dam break problem and flows in swash zones. You and Yin (2007) measured shear stress using shear plate under regular waves. When using a shear plate, the force measured by the shear plate includes the bed shear stress and the pressure gradient force from the wave. Linear wave theory is often used to estimate (Rankin and Hires, 2000) and eliminate the pressure gradient from the total force so as to obtain the bed shear stress. However, the total stress applied to the upper sediment layers is possibly equally important in terms of sediment motion (e.g. plug flow), slope stability and load carrying capacity. Therefore, the total stress measured by the shear plate is also useful. In order to predict the potential impact of tsunami propagation over the continental slope and shelf, numerical modelling is required. In this study, numerical modeling of the propagation of a solitary wave in the wave flume is performed using a two 2D depth averaged hydrodynamic model. This paper presents comparisons of the modelled and measured waveforms, flow velocities, and bed stress measurements under three types of waves, viz., solitary, bore and Leading Depression N (LDN) wave.

2. Study region and tsunami hazard

Australia has a vast maritime jurisdiction and additional 2.5 million square kilometers have been recently confirmed by the United Nations (UN) Commission on the Limits of Continental Shelf, apart from an additional area beyond 200 nautical miles, which is known as extended continental shelf. The majority of the national oil & gas reserves are present in the offshore regions. These offshore reserves have been explored and exploited for many decades, and of late, exploration is being extended to deeper waters. Most of these offshore reserves are along the western and north-western region of Western Australia, with more limited current exploration on the east and southern Australian coasts (Figure 1). The bathymetry offshore of the North West Australian coast is complex, with steep shelf slopes, ridges, canyons, plateaus, reefs, etc. Subsea pipelines often laid on the seabed are used to transport the oil and gas from these offshore reserves to the coast. These pipelines traverse complex ocean bathymetry with uneven topography and changing slopes, thereby are subjected to structural, hydrodynamic and other forces. Typical seabed profiles of the continental slope and shelf along the northwest Australian coast, shown in Figure 1, indicate that the subsea pipelines have to be laid over slopes varying between 1:7.5 to 1:35 in the steeper regions and 1:200 over the flat regions (Figure 2.). As the seabed is not always flat and the cost involved in preparing the seabed for laying of pipelines, they are routed through most economical and safe regions. These pipelines are often designed to withstand the operational and installation forces that they encounter as well as loads arising from varying spans, vibrations, etc. However, the hydrodynamic loading on these pipelines due to debris flow or pressure gradients that these pipelines encounter may not be properly assessed due to lack of information on such phenomena. Often an extra factor of safety is considered to encompass all other unknown loads, which might be an over design of the pipelines. Assessment of the conditions for initiation of debris flow during a tsunami would be highly desirable to improve the understanding of the hazards associated with the subsea pipelines. The steep surface gradients of breaking tsunami may induce bed stresses and temporary liquefaction of the seabed in the nearshore zone. Further offshore, the bed shear stresses may trigger submarine landslides and debris flows, particularly during the drawdown phase at the shelf edge.

Considering the geo-tectonic setting of Australia, wherein active crustal subduction, high seismicity and volcanic activity occur all around the continent, threat of tsunami is very high to this region (Dominey-Howes et al., 2007). Earthquakes of a magnitude greater than 6 and with focal depths less than 30 km show high activity all around the Australia coast. A compilation of geological and historical records of tsunami in Australia reveal that about 47 events since 1858 and about 10 palaeo-tsunami events have affected the Australian coast (Dominey-Howes et al., 2007). Burbidge and Cummins (2007) assess the tsunami threat to Western Australia (WA) coast from earthquakes along the Sunda trench (Indonesia) and state that the occurrence of the Sumatra-Andaman tsunami on 26 December 2004 has raised concern amongst Australian emergency management authorities about lack of information on the tsunami threat to Australia. In view of

the unknown threat from this region as well as other adjoining tsunamigenic regions, the offshore installations are at unknown risk. The subduction zone south of Indonesia (the Sunda arc) is one major tsunamigenic source from which the WA coast can expect high risks (Satake et al., 1992). The far field tsunami sources that could have an impact on the Australian coast are along the South America, Pacific and Southern oceans. In view of the high tsunami risks involved in this part of the world, the importance of the offshore oil & gas industry and the ultra-long tiebacks being considered for new fields, it is essential to understand the effect of tsunamis on the seabed. While tsunami have not traditionally been considered in the design process, the flow velocity induced at the sea bed at the edge of the continental shelf is typically more severe than those induced by tropical cyclones (Table 1). Measured maximum wave height of 20 m with a wave period of 12 s for tropical cyclone Olivia (Buchan et al., 2002) and a typical tsunami height of 1 m and 30 – 40 minutes period are considered to illustrate the flow velocities related to tsunamis. Even at large depths, considerable amount of flow velocities can be seen during tsunami propagation. Such flows may be amplified locally by focusing and submarine canyons, the latter of which may be pipeline routes.

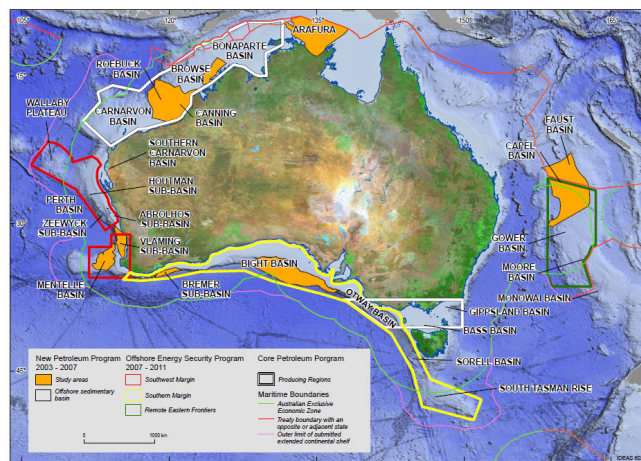


Figure 1. Frontier basins targeted for further exploration studies (Source: Geoscience Australia)

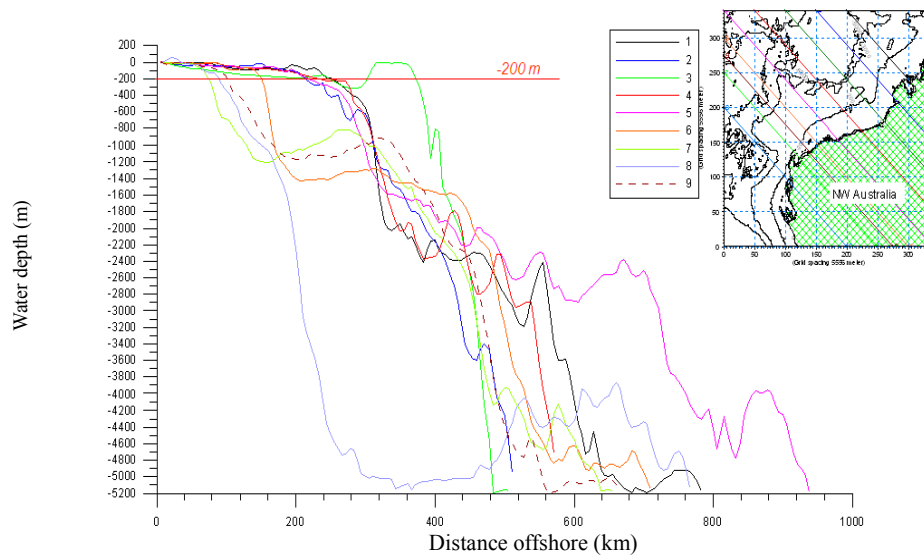


Figure 2. Cross section profiles of continental shelf off North West Australia

Table 1. Wave parameters for selected solitary waves generated in laboratory that are comparable with the theory

Parameters	Cyclone (shallow)	Cyclone (deep)	Tsunami-1 (shallow)	Tsunami-2 (shallow)	Tsunami-1 (deep)	Tsunami-2 (deep)
Wave height (m)	20	20	1	1	1	1
Wave period (s)	12	12	1800	2400	1800	2400
Water depth (m)	125	1000	125	125	1000	1000
Bottom velocity [@] (m/s)	0.315	0.000	0.887	1.024	0.186	0.215
Bottom pr coefficient [@] (K_p)	0.060	0.000	0.999	0.999	0.999	0.999
Bottom pressure (= $K_p \cdot \rho \cdot g \cdot \text{wave Ht.}$) (Pa)	6033	0	5028	5028	5028	5028

@Using Linear wave calculator (<http://www.coastal.udel.edu/faculty/rad/wavetheory.html>)

3. Methodology

Laboratory experiments and numerical modeling of wave propagation is carried out to estimate the total bed stress and shear stress under tsunami type waves. Laboratory experiments were carried out at the Gordon McKay hydraulics laboratory of the University of Queensland, Australia. A schematic plot of the wave flume setup with the instruments is shown in Figure 2. A long-wave wave generator has been fabricated and installed in a wave flume 0.85 m wide, 0.75 m deep and with a wave propagation distance of more than 10 m. The wave generation is performed through a hydraulic pump. The input signal or wave form is provided as a DC electrical voltage signal to the hydraulic pump which moves the wave paddle accordingly. This specially fabricated wave generator has a stroke length of over 1 m. A shear cell, described in detail in Barnes et al (2009, 2006), is used to measure the shear stresses under various wave forms. The displacement of the shear plate in the shear cell is measured as an estimate of the force since the force applied over the shear plate translates into the horizontal movement of the shear plate. The horizontal displacement vector of the shear plate is measured by a single Indikon Eddy-current proximity probe (model XLG-1B) aligned perpendicular to a target plate attached to the underside of the shear plate. The shear cell is placed flush with the wave flume bed along with pressure transducers on either side of the shear cell to measure the pressure which can be used to eliminate the pressure force due to the wave. Microsonic (MS) Mic+25/IU/TC acoustic displacement sensors with an accuracy of 0.18 mm and response time of 50 ms (Microsonic, 2005) are used to measure the surface displacement or the wave heights. Instantaneous velocities were measured using a 2D side-looking SonTek micro Acoustic Doppler Velocimeter (ADV) 16 MHz (Sontek, 2001). The ADV acoustic sensor is located close to the bed with a horizontal distance to sample volume of 0.05 m. The ADV is positioned to the side and central to the shear plate so that the sample volume was above the shear plate. The horizontal velocity component (U_x) was aligned longitudinally to the flow direction and the transverse component (U_y) orientated normal to the channel side wall.

Wave profiles were generated using appropriate wave theory for the solitary and leading depression 'N' (LDN) waves and the bores were generated by providing higher energy to the solitary waves and allowing them to break and run as a bore. Goring's method of solitary wave generation was adopted and solitary wave forms of various heights were generated (Goring, 1979). All the runs considered in this particular paper are run for a water depth of 15.5 cm. The wave data was discretized and provided to the wave generator at a rate of 100 Hz. Data transmission and acquisition is carried out by in-house software written in Microsoft Visual Basic and the digital data transmission is carried out through National Instruments data acquisition card.

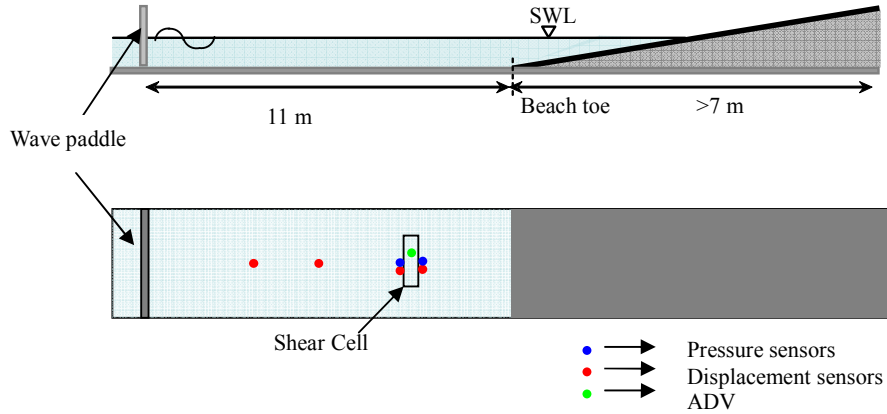


Figure 2. Schematic setup of instruments in wave flume

The general form of the solitary wave equation used is presented in equation (1). Leading depression ‘N’ waves were generated using the formulation provided in Tadepalli and Synolakis (1994). The general form of the equation is presented in equation (2).

$$\eta(0, x) = \text{Sech}^2 \left[\sqrt{\left(\frac{3H}{4d^3} \right)} (x - X_1) \right] \quad (1)$$

$$\eta(0, x) = \varepsilon H (x - X_2) \text{Sech}^2 \left[\sqrt{\left(\frac{3H}{4} \right)} (x - X_1) \right] \quad (2)$$

where, $\eta(0, x)$ is the surface elevation at a distance x , H is the maximum wave amplitude, d is water depth, X_1 and X_2 are limits of wavelength, ε is scaling factor (<1).

The shallow water equations (3), (4) and (5) are fundamental equations used in the depth averaged 2D numerical models that are used for tsunami propagation modeling. Additional terms of Coriolis force, wind stress, turbulence, atmospheric pressure, etc., are added on to these fundamental equations whenever these terms are deemed to have a major contribution.

$$\frac{\partial \eta}{\partial t} + u \frac{\partial (h + \eta)}{\partial x} + v \frac{\partial (h + \eta)}{\partial y} = 0 \quad (3)$$

$$\frac{\partial u}{\partial t} + u \frac{\partial u}{\partial x} + v \frac{\partial u}{\partial y} + g \frac{\partial \eta}{\partial x} + \frac{\tau_x}{\rho} = 0 \quad (4)$$

$$\frac{\partial v}{\partial t} + u \frac{\partial v}{\partial x} + v \frac{\partial v}{\partial y} + g \frac{\partial \eta}{\partial y} + \frac{\tau_y}{\rho} = 0 \quad (5)$$

where, h is the undisturbed water depth, η is vertical displacement above still water level, u and v are depth averaged water particle velocity components in the cross-shore x and alongshore y directions, τ_x and τ_y are bottom friction coefficients in x - and y - directions.

The bottom friction terms are most often written in terms of Manning’s ‘ n ’ or Chezy’s coefficient, ‘ C ’, which are related as $C = h^{1/6} / n$. The bottom friction terms are expressed as follows:

$$\frac{\tau_x}{\rho} = \frac{gn^2}{h^{4/3}} u \sqrt{u^2 + v^2} = \frac{g}{C^2 h} u \sqrt{u^2 + v^2} \quad (6)$$

$$\frac{\tau_y}{\rho} = \frac{gn^2}{h^{4/3}} v \sqrt{u^2 + v^2} = \frac{g}{C^2 h} v \sqrt{u^2 + v^2} \quad (7)$$

Numerical modeling of the wave flume was carried out using a depth averaged two-dimensional hydrodynamic/flow model (MIKE21-HD) developed by the DHI Water Health and Environment, Denmark (DHI, 2007). Depth integrated shallow water equations (continuity and momentum equations) are solved in x-y spatial frame, including the Coriolis force, bed roughness in terms of Manning's coefficient, and eddy-viscosity. Measured wave data from the laboratory experiments were provided as input to the numerical model in order to calibrate the model and also to extract the roughness coefficients for estimating the shear stress. From the bottom friction terms as represented in (6) and (7) the bed shear stress can be estimated once the flow velocities and fluxes are matched with the measured flow data for a given bed roughness parameter. The model domain used for the numerical modeling of the flume consisted of square grids of 20 cm over a length of 8 m and width of 0.8 m. Only the region between the first wave gauge and the beach slope was considered in the model as the region beyond the beach and before the first wave gauge do not contribute anything significant in the model results. The model results for a particular case of the experiment were simulated. In order to match the measurements along the flume, with the input wave from the first gauge, various values of bed resistance were tried and the bed roughness corresponding to the best match of the model results with the measurements was obtained from different trials.

The bed roughness or friction factors estimates from the Reynolds number of all the solitary waves generated in the laboratory was estimated based on the study carried out by Ippen and Mitchel (1957). Also the friction factor that was required to match the model results with the measurements was compared for a solitary wave case. The Reynolds number, \Re , as per Ippen and Mitchel (1957), assuming small amplitude theory, for the entire wave is given by equation (8). The estimated friction factors using Reynolds number is given in equation (9) and based on the shear stress, τ_o , and bottom velocity, U , is given in equation (10).

$$\Re = 1.54H \frac{\sqrt{gH}}{\nu} \quad (8)$$

$$C_f = \sqrt{\frac{1.2}{\Re}} \quad (9)$$

$$C_f = \frac{2\tau_o}{\rho U^2} \quad (10)$$

$$U = \frac{cN}{2} \text{Sech}^2 \left(\frac{M}{2d} \right) \quad (11)$$

$$\eta = H * \text{Sech}^2 \sqrt{\frac{3H}{4d}} * \frac{x}{d} \quad (12)$$

where, H is the wave amplitude, g is acceleration due to gravity, ν is viscosity of water, C_f is the friction factor, ρ is density of water, c is wave celerity, M & N are dimensional parameters of relative water depth as given by McCowan-Munk theory, d is water depth.

In order to ascertain the fact that the measured wave parameters are consistent with the theory, measured data of wave induced velocities near the bed and the wave celerity were compared. Also, the measured wave profiles were compared with the Boussinesq solitary wave profile (12). Most of the

measured profiles matched well with the theory for a given relative depth, although some do not, particularly those close to breaking. .

4. Results and discussion

4.1. Wave flume experiments

Typical wave profile, total bed, bottom pressure and velocity under a solitary wave and a broken solitary bore in the laboratory are shown in Figure 3. The different wave heights, corresponding stresses, and other parameters that were measured and computed for selected solitary waves that compared well with the theoretical solitary wave profile are presented in Table. 2. Other broken solitary waves were also used in the estimation of friction coefficient and near bed velocity. Though the broken waves and LDN waves were generated in the laboratory these are not discussed in detail in this paper except that the wave profile at different propagation distances from the wave paddle are presented in Fig. 3.

Wave propagation of the Solitary wave, bore and LDN waves presented in Figure 3 show that the wave develops into a stable form by the time it reaches the shear cell located at 8.6 m from the paddle and thereafter maintains its shape over the shear cell, which can be seen from the wave profile measured at 8.7 m from the paddle. Compared to the bores and LDN waves, solitary waves generated were found to maintain the wave amplitude almost through the entire propagation. However, the LDN waves were not found to have a stable form from the generation point to the shear cell. Therefore, the data pertaining to LDN waves are not considered further in this paper.

The pressure distribution below the solitary wave was observed to follow the hydrostatic law and therefore no further attempt is made to analyse the pressure signals measured from the pressure transducers, although the data pertaining to these are available for further use, if required. The velocity measured using ADV is synchronized with the wave measurements and thereby the wave synchronous flow velocity data is measured. The velocity profile closely follows the wave profile indicating that there is no change of direction of flow under the crest of the wave. However, the total shear stress as measured from the shear cell shows that the shear stress changes its sign during the deceleration phase as the fluid particle velocity changes its direction in the boundary layer, which has been observed by earlier researchers e.g., (Ippen and Mitchell, 1957, Liu et al., 2007). This shows that the present measurements are in agreement with similar measurements made by earlier researchers and the theories that had been adopted could be applied to these measurements as well. For the solitary wave profile presented in Fig. 4, the phase lag between the maximum amplitude and the maximum bed stress was about 0.325 s which corresponds to a phase angle of 45° whereas for the solitary bore it was 0.175 s (about 57°). Hence, pressure gradient terms dominate the total bed stress at this wave steepness. Further work is required to separate the pressure gradient from the total stress to calculate the friction factor.

The wave induced flow velocity near the flume bed measured by ADV was compared with theoretical wave orbital velocity as given by equation (11). The comparison shows that irrespective of breaking or non-breaking solitary wave, measured flow velocities more or less are comparable with the theoretical values except for the higher velocities beyond 45 cm/s wherein the computed velocities are higher than the measurements (Figure 5a). This could be due to the breaking of waves during high velocities and loss of energy and momentum in the wave profile. However, when only the non-breaking solitary waves that match their profile with the solitary wave theory are considered, there is an improvement in the comparison with the theoretical values (Figure 5b). Also the flow velocities with respect to the wave steepness are found to increase exponentially (Figure 6).

The total bed stress measured using the shear cell presented with respect to the wave steepness indicates that the shear stress depends linearly on the wave steepness for the solitary waves that are non-breaking and that follow the solitary wave theory (Figure 7a). However, for the breaking solitary bores (Figure 7b) the shear stress did not show any significant correlation with the wave steepness.

4.2. Numerical model results

Numerical modeling was performed for solitary wave propagation using DHI's MIKE21 hydrodynamic Flow Model using rectangular grids and Cartesian system of coordinates and one example is shown below. Measured wave height and flow velocity were provided as input data to the model (Figure 10) and the flow pattern along the flume was simulated. The wave height or water surface elevation near the shear cell and other two locations were extracted from the model and compared with the measurements for the same

experimental run. The bed friction and the eddy viscosity parameters were varied until a reasonable match of the model results and experimental data was achieved.

The wave height or water surface profiles obtained from the model results compared with the measurements are shown in Figure 11. The bed friction parameter used for this run corresponds to a Manning number of 0.03125 and eddy viscosity coefficient of 0.5 using Smagorinsky's formulation (Smagorinsky, 1963). From the preliminary model results obtained, it is observed that the model is capable of reproducing the surface elevation propagation to a reasonable extent. However, the model results are ahead of the measurements which could be resolved by modifying the bed friction coefficient and eddy viscosity terms which are calibrating parameters in this numerical modeling. The propagation of solitary waves is feasible using a 2D hydrodynamic model, although robust Boussinesq models are available, which require higher computational efforts. Further model investigations for other experimental runs are being studied to ascertain the usability of the hydrodynamic model for solitary wave propagation and thereby adopting the numerical model for simulating various tsunami type wave forms (bore and Leading Depression N waves or Leading Elevation N waves), the results of which will be presented in a later paper.

5. Conclusions

This paper concerns a study consisting laboratory experiments on propagations both non-breaking and broken Solitary waves in a wave flume and an attempt towards numerical modeling of solitary wave propagation using MIKE21-2D hydrodynamic flow model. The application is to tsunami propagation over the steep continental slope and the nearshore zone where breaking of tsunami wavefronts may occur. The bed stress in these regions is important in the stability of submarine sediments. Laboratory experiments were performed to obtain total shear stresses under tsunami-type breaking and non-breaking solitary waves. The total stress comprises arises from a pressure gradient force and a skin friction shear stress, and the pressure gradient force is important in terms of the total stress exerted on the sediment bed. The measured flow velocities and the computed velocities based on solitary wave theory are found to be consistent for non-breaking solitary waves whereas the velocities measured from broken or breaking solitary wave was less than the computed flow for similar wave amplitudes. Modeling of the solitary wave propagation using a depth averaged numerical model indicate that it is possible to model the solitary wave propagation to a reasonable extent, thereby the total bed stresses and the bed friction coefficients can be estimated for various wave forms.

Table 2. Wave parameters for selected solitary waves generated in laboratory that are comparable with the theory

H (cm)	H/depth	L (computed) (cm)	T (s)	U (measured) (cm/s)	Shear stress (10^{-1} N m^{-2})	Reynolds No.	U (computed) (cm/s)
1.41	0.09	373.27	2.90	10.36	0.49	8058.59	10.30
1.58	0.10	352.52	2.72	12.26	0.55	9566.73	11.44
2.61	0.17	274.11	2.06	18.29	1.74	20350.05	17.93
3.31	0.21	243.41	1.79	23.34	1.91	29059.89	21.99
3.48	0.22	237.32	1.74	23.51	1.08	31357.51	22.95
5.07	0.33	196.80	1.39	32.07	1.87	54982.49	31.17
5.34	0.34	191.74	1.34	33.05	1.53	59450.37	32.48
6.43	0.41	174.67	1.19	38.45	2.32	78645.10	37.53
7.02	0.45	167.17	1.12	41.82	2.66	89714.14	40.12
7.44	0.48	162.38	1.08	42.88	1.64	97882.68	41.90
8.02	0.52	156.42	1.03	43.93	3.19	109510.13	44.28
8.57	0.55	151.27	0.98	42.17	1.61	121079.23	46.49
9.74	0.63	141.95	0.90	52.28	3.73	146529.84	50.93
10.00	0.64	140.09	0.89	47.56	1.93	152431.61	51.89

(H – wave amplitude in front of shear cell, L – wave length, T – wave period, U – near bed velocity)

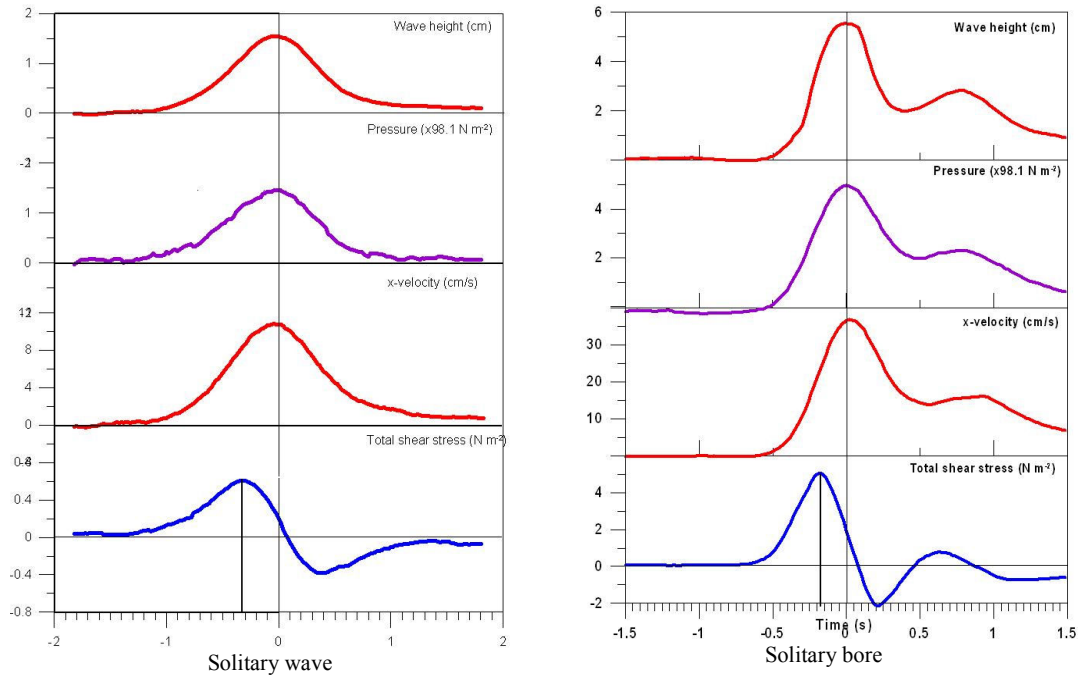


Figure 3. Plot showing wave profile, pressure trace, measured near-bed velocity and shear stress for (a) Solitary wave and (b) Solitary bore

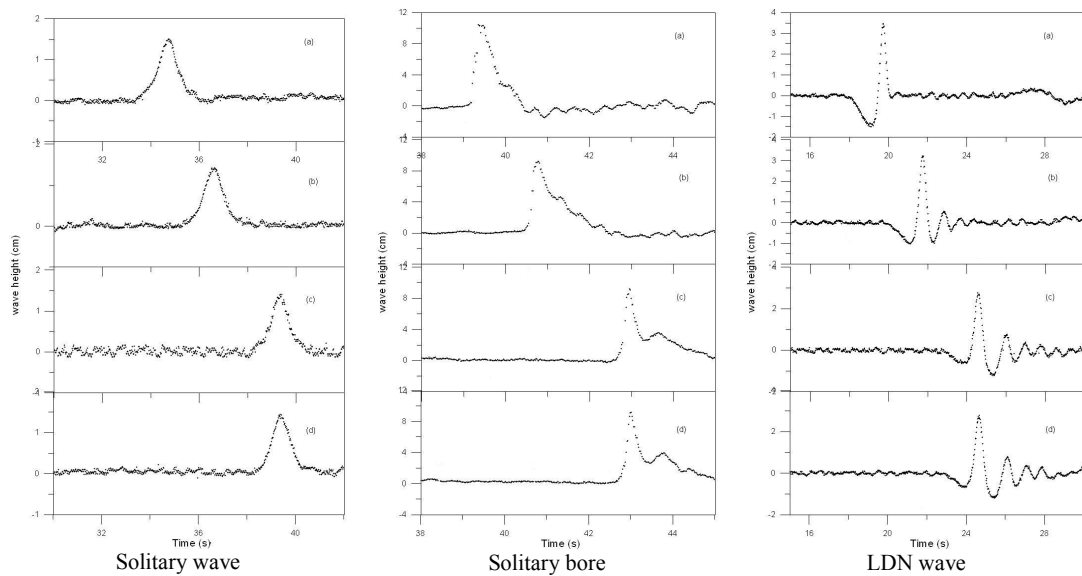


Figure 4. Propagation of Solitary wave, Solitary bore and Leading Depression N wave. (a) wave profile at 2.6 m from wave paddle (b) wave profile at 6.1 m from wave paddle (c) wave profile at 8.6 m from wave paddle and (d) wave profile at 8.7 m from paddle

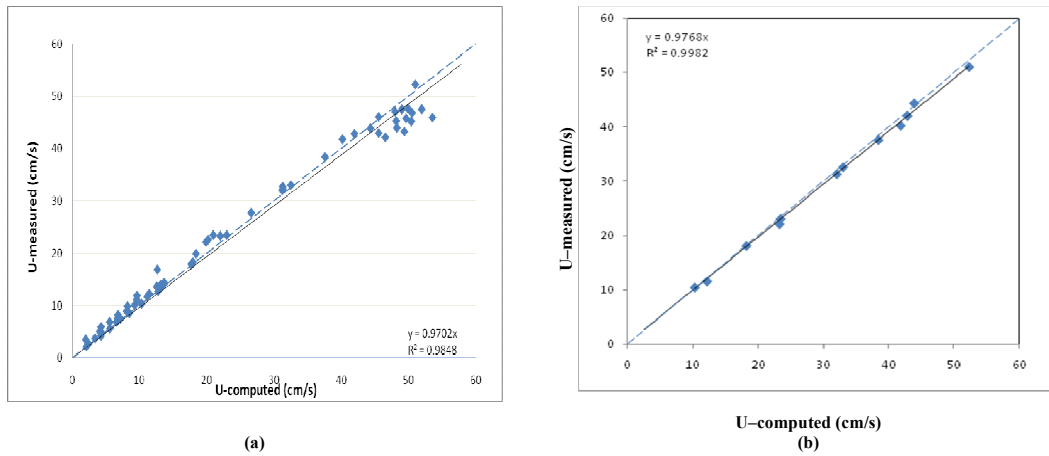


Figure 5. Plot showing relation between measured and computed near bed velocity (a) for all solitary type waves; solid line represents the best fit linear curve and the dashed line is the line of equality (b) only for non-breaking Solitary waves

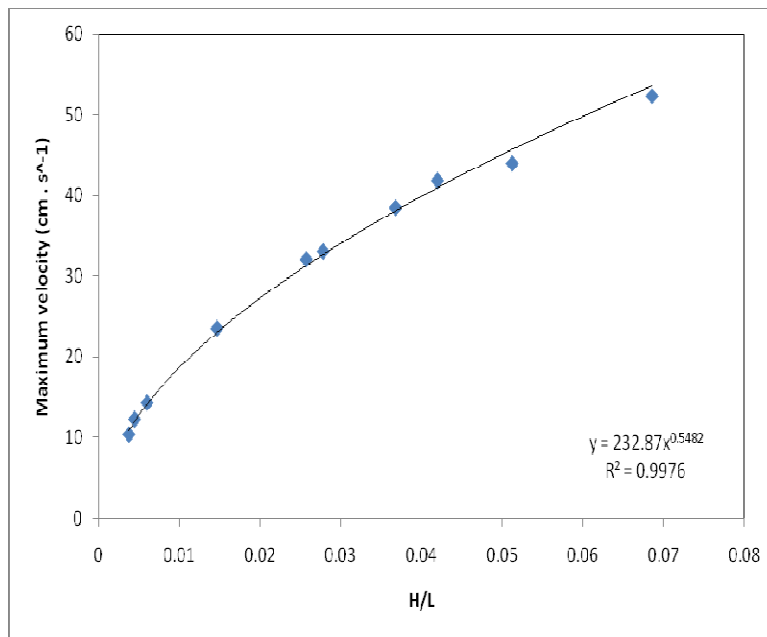


Figure 6. Plot showing relation between non-breaking solitary wave steepness and maximum velocity

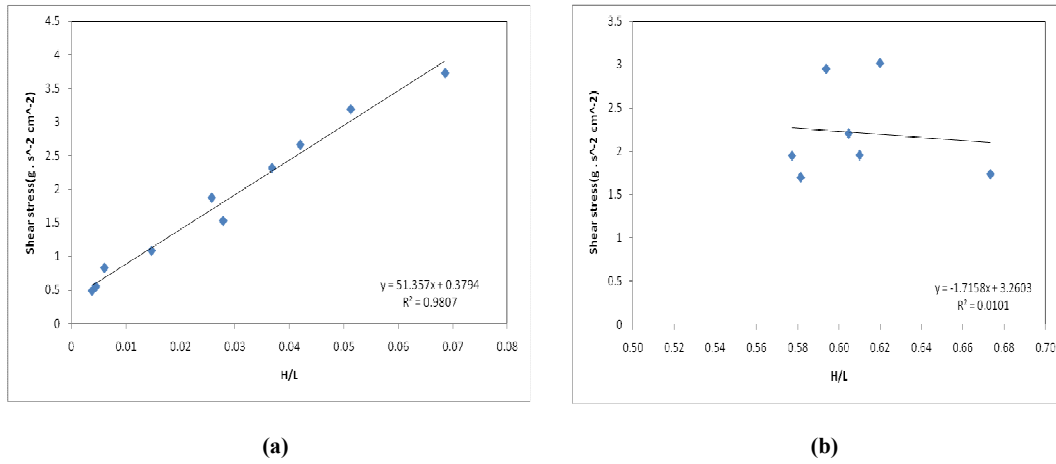


Figure 7. Plot showing relation between wave steepness and total shear stress for (a) non-breaking solitary and (b) broken solitary waves

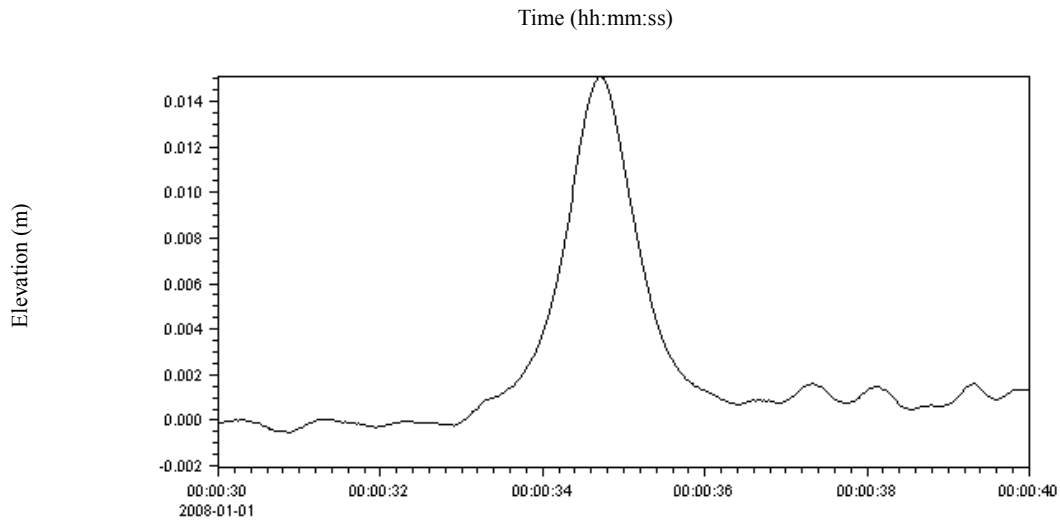


Figure 8. Wave input data to the numerical model

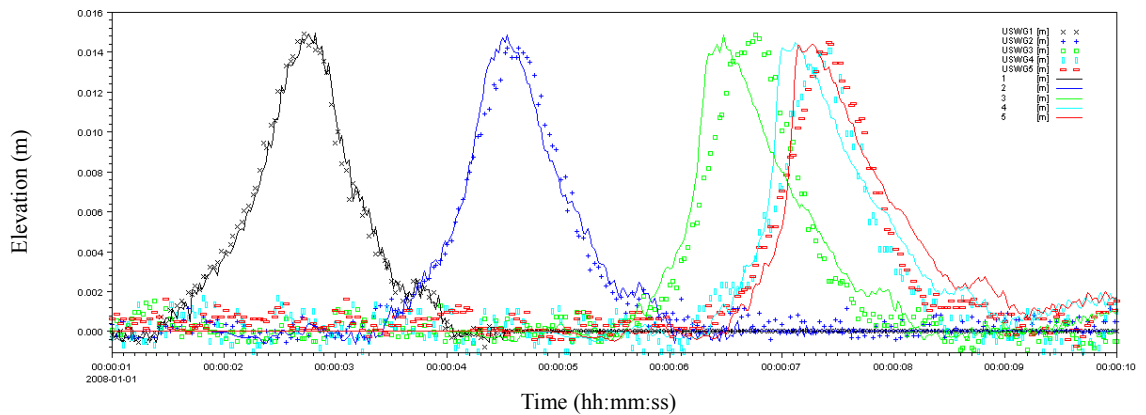


Figure 9. Wave profile comparison between the numerical model and measurements

Acknowledgements

This paper is a part of the research project supported by CSIRO's Flagship Cluster Grant under Wealth from Oceans – Pipeline Hazards program. Authors appreciate the cooperation and help rendered by Graham Illidge, Clive Booth and Amhed Ibrahim in the wave flume experiments. First author is an Endeavour IPRS scholar at the University of Queensland and he acknowledges the support of his parent organization, National Institute of Oceanography, Goa, India, a constituent laboratory of the CSIR-India.

References

- BARNES, M. P. & BALDOCK, T. E. (2006) Bed shear stress measurements in dam break and swash flows. *International Conference on Civil and Environmental Engineering*. The University of Hiroshima, Japan.
- BARNES, M. P. & BALDOCK, T. E. (2007) Direct Bed Shear Stress Measurements in Laboratory Swash. *Journal of Coastal Engineering*, SI 50, 641-645.
- BARNES, M. P., O'DONOGHUE, T., ALSINA, J. M. & BALDOCK, T. E. (2009) Direct bed shear stress measurements in bore-driven swash. *Coastal Engineering*, In Press, Corrected Proof.
- BUCHAN, S. J., TRON, S. M. & LEMM, A. J. (2002) Measured tropical cyclone seas. *Seventh International workshop on wave hindcasting and forecasting*. Banff, Alberta, CANADA.
- BURBIDGE, D. & CUMMINS, P. (2007) Assessing the threat to Western Australia from tsunami generated by earthquakes along the Sunda Arc. *Natural Hazards*, 43, 319-331.
- CHANG, K.-A. & LIU, P. L.-F. (1998) Velocity, acceleration and vertical vortex under a breaking wave. *Physics of Fluids*, 10, 327-329.
- CHANG, K.-A. & LIU, P. L.-F. (1999) Experimental investigation of turbulence generated by breaking waves in water of intermediate depth. *Physics of Fluids*, 11, 3390-3400.
- COWEN, E. A. & MONISMITH, S. G. (1997) A hybrid digital particle tracking velocimetry technique. *Experiments in Fluids*, 22, 199-211.
- COWEN, E. A., SOU, I. M., LIU, P. L.-F. & RAUBENHEIMER, B. (2003) Particle image velocimetry measurements within a laboratory-generated swash zone. *Journal of Engineering Mechanics*, 129, 1119-1129.
- DHI (2007) *Hydrodynamic Module - Scientific Documentation*, DHI, Denmark.
- DOMINEY-HOWES, D., CUMMINS, P. & BURBIDGE, D. (2007) Historic records of teletsunami in the Indian Ocean and insights from numerical modelling. *Natural Hazards*, 42, 1-17.
- GÍSLASON, K. F., J. DEIGAARD, R. SUMER, B. M. (2009) Flow understanding waves: Part 1. Shear stress distribution, energy flux and standing waves. *Coastal Engineering*, In Press, Corrected Proof.
- GORING, D. G. (1979) Tsunamis - The propagation of long waves on to a shelf. *Division of Engineering and Applied Science*. Pasadena, California Institute of Technology.
- HOLMEDAL, L. E., MYRHAUG, D. & RUE, H. (2003) The sea bed boundary layer under random waves plus current. *Continental Shelf Research*, 23, 717-750.
- HUANG, C.-J. & DONG, C.-M. (2001) On the interaction of a solitary wave and a submerged dike. *Coastal Engineering*, 43, 265-286.
- IPPEN, A. T. & MITCHELL, M. M. (1957) The damping of the solitary wave from boundary shear measurements. Massachusetts Institute of Technology.
- JENSEN, B. L., SUMER, B. M. & FREDSOE, J. (1989) Turbulent oscillatory boundary layers at high Reynolds numbers. *Journal of Fluid Mechanics*, 206, 265-297.
- LIANG, B.-C., LI, H.-J. & LEE, D.-Y. (2008) Bottom Shear Stress Under Wave-Current Interaction. *Journal of Hydrodynamics, Ser. B*, 20, 88-95.
- LIN, J. C. & ROCKWELL, D. (1994) Instantaneous structure of a breaking wave. *Physics of Fluids*, 6, 2877-2879.
- LIN, J. C. & ROCKWELL, D. (1995) Evolution of a quasi-steady breaking wave. *Journal of Fluid Mechanics*, 302, 29-43.
- LIN, P. & ZHANG, W. (2008) Numerical simulation of wave-induced laminar boundary layers. *Coastal Engineering*, 55, 400-408.
- LIU, P. L.-F., DAVIS, M. H. & DOWNING, S. (1996) Wave-induced boundary layer flows above and in a

- permeable bed. *Journal of Fluid Mechanics*, 325.
- LIU, P. L. F., PARK, Y. S. & COWEN, E. A. (2007) Boundary layer flow and bed shear stress under a solitary wave. *Journal of Fluid Mechanics*, 574, 449-463.
- LIU, P. L. F., SIMARRO, G., VANDEVER, J. & ORFILA, A. (2006) Experimental and numerical investigation of viscous effects on solitary wave propagation in a wave tank. *Coastal Engineering*, 53, 181-190.
- MICROSONIC (2005) Instruction Manual. IN GMBH, M. (Ed.). Dortmund, Germany.
- RANKIN, K. L. & HIRES, R. (2000) Laboratory measurement of bottom shear stress on a movable bed. *Journal of Geophysical Research*, 105.
- SATAKE, K., YOSHIDA, Y. & ABE, K. (1992) Tsunami from the mariana earthquake of april 5, 1990 - its abnormal propagation and implications for tsunami potential from outer-rise earthquakes. *Geophysical Research Letters*, 19, 301-304.
- SLEATH, J. F. A. (1987) Turbulent oscillatory flow over rough beds. *Journal of Fluid Mechanics*, 182.
- SMAGORINSKY, J. (1963) General circulation experiments with the primitive equations. *Monthly weather review*, 91, 91-164.
- SONTEK (2001) *Sontek/YSI ADVField/Hydra Acoustic Doppler Velocimeter (Field) Technical Documentation*, San Diego, USA.
- SUMER, B. M., ARNSKOV, M. M., CHRISTIANSEN, N. & JORGENSEN, F. E. (1993) Two-component hot-film probe for measurements of wall shear stress. *Experiments in Fluids*, 15, 380-384.
- SYNOLAKIS, C. E. & BERNARD, E. N. (2006) Tsunami science before and beyond Boxing Day 2004. *Philosophical Transactions - A Math Physics Engineering Science*, 364, 2231-2265.
- TADepALLI, S. & SYNOLAKIS, C. E. (1994) THE RUN-UP OF N-WAVES ON SLOPING BEACHES. *Proceedings of the Royal Society of London Series a-Mathematical Physical and Engineering Sciences*, 445, 99-112.
- YOU, Z.-J. & YIN, B. S. (2007) Direct Measurement of Bottom Shear Stress under Water Waves. *Journal of Coastal Research*, SI 50, 1132 - 1136.